

Induced gravitational waves for arbitrary higher orders: vertex rules and loop diagrams in cosmological perturbation theory

Jing-Zhi Zhou ^{1,2,*} Yu-Ting Kuang ^{3,4} Di Wu ^{3,4} H. Lü ^{1,2} and Zhe Chang ^{3,4}

¹*Center for Joint Quantum Studies and Department of Physics,
School of Science, Tianjin University, Tianjin 300350, China*

²*Joint School of National University of Singapore and Tianjin University,
International Campus of Tianjin University, Binhai New City, Fuzhou 350207, China*

³*Institute of High Energy Physics, Chinese Academy of Sciences, Beijing 100049, China*

⁴*University of Chinese Academy of Sciences, Beijing 100049, China*

Gravitational waves induced by primordial perturbations serve as crucial probes for studying the early universe, providing a significant window into potential new physics during cosmic evolution. Due to the potentially large amplitudes of primordial perturbations on small scales, the contributions of high-order cosmological perturbations (CPs) are highly significant. We propose a vertex approach applicable to the study of induced gravitational waves for arbitrary higher orders. Using the vertex approach and tree diagrams, we can directly derive the explicit expressions of higher-order induced gravitational waves without involving the complex and lengthy calculations of higher-order CPs. Correlations between different tree diagrams correspond to the loop diagrams of two-point correlation functions of induced gravitational waves. Our investigation reveals that one-particle reducible (1PR) diagrams impact tensor-scalar induced gravitational waves (T-SIGWs) while leaving scalar induced gravitational waves (SIGWs) unaffected.

Introduction.—Our universe originated from primordial perturbations generated during the inflationary epoch [1–3]. These perturbations, serving as the initial conditions for cosmic evolution, encode crucial physical insights into the early universe. By leveraging current cosmological observations—such as cosmic microwave background (CMB), large scale structure (LSS), and primordial black holes (PBHs)—we can discern the physical properties of primordial perturbations across various scales [4–7]. In June 2023, several international pulsar timing array (PTA) collaborations, such as NANOGrav [8], PPTA [9], EPTA [10], and the CPTA [11], provided evidence for the existence of a stochastic gravitational wave background (SGWB) in the nHz frequency range. This breakthrough provides a fresh avenue for investigating potential new physics during the early universe and characterizing the physical properties of small-scale primordial perturbations. Specifically, primordial perturbations generated during the inflationary epoch, upon re-entering the horizon after inflation, can induce gravitational waves (GWs) with discernible effects [12]. Current PTA observational data suggest that induced GWs are among the most likely sources contributing to the SGWBs [13]. The imprint of potential new physics during inflation and the nature of small-scale primordial perturbations are encoded in today’s PTA observations [14–18].

The investigation into scalar induced gravitational waves (SIGWs) on small scales is inspired by research on the impact of second-order tensor and vector perturbations induced by first-order scalars on CMB polarization [19]. Building on previous research on second-order perturbations at the CMB scale, Refs. [20–22] studied the second-order GWs induced by large-amplitude primordial scalar perturbations on small scales and calculated the corresponding energy density spectrum. In the past decade, researches on second-order SIGWs has been extended to PBHs [23–37], gauge issue [38–49], primordial non-Gaussianity [50–63], different epochs of the Universe [64–79], and damping effect [80–83].

As a measurable quantity within PTA experiments, the energy density spectrum of SIGWs can be expressed as $\Omega_{\text{GW}}(k) = A_{\zeta}^2 \Omega_{\text{GW}}^{(2)}(k) + A_{\zeta}^3 \Omega_{\text{GW}}^{(3)}(k) + \dots$, where the perturbation expansion parameter A_{ζ} represents the amplitude of the power spectrum of primordial curvature perturbation. While previous studies mainly focused on second-order SIGWs, recent research emphasizes the impact of third-order SIGWs on current PTA observations [84–89]. Disregarding higher-order effects will inevitably lead to deviations in the primordial perturbation parameters derived from the analysing of PTA data. Consequently, there is a compelling physical motivation to meticulously compute or rigorously estimate the higher-order effects arising from induced GWs. However, computing higher-order induced GWs remains an arduous endeavor, requiring rigorous derivation and solution of higher-order cosmological pertur-

* zhoujingzhi@tju.edu.cn

bation (CP) equations, followed by the evaluation of relevant two-point correlation functions [90–92]. Conventional methods for studying arbitrary higher-order induced gravitational waves appear almost unfeasible.

We present a systematic framework for investigating higher-order induced GWs, introducing both vertex and loop diagram approaches. These approaches empower us to explore arbitrary higher-order scenarios. By utilizing the vertex approach, the explicit expression for higher-order induced GWs can be derived with pen and paper, without involving thousands of terms from complex and lengthy calculations of higher-order CPs. In the loop diagram approach, we can use different types of loop diagrams to calculate the two-point correlation function of induced GWs. Our investigation reveals that one-particle reducible (1PR) diagrams affect tensor-scalar induced gravitational waves (T-SIGWs) while leaving SIGWs unaffected [93–95].

Equations of motion.—The perturbed metric in the Friedmann-Lemaître-Robertson-Walker (FLRW) spacetime with Newtonian gauge takes the form

$$ds^2 = a^2 \left(-(1 + 2\phi) d\eta^2 + 2V_i d\eta dx^i + ((1 - 2\psi) \delta_{ij} + h_{ij}) dx^i dx^j \right). \quad (1)$$

The CPs A (where $A = \phi, \psi, V_i$, and h_{ij} in Eq. (1)) can be expressed as $A = \sum_{n=1}^{\infty} \frac{1}{n!} A^{(n)}$. Within the specified metric perturbation framework, we can conveniently investigate the influence of different lower-order perturbations on higher-order induced GWs. For instance, considering second-order GWs $h_{ij}^{(2)}$ induced by first-order scalar perturbation $\phi^{(1)}$, we set $\phi = \phi^{(1)}$, $h_{ij} = \frac{1}{2} h_{ij}^{(2)}$, and $\psi = V_i = 0$. Namely,

$$ds^2 = a^2 \left(-(1 + 2\phi^{(1)}) d\eta^2 + \left(\delta_{ij} + \frac{1}{2} h_{ij}^{(2)} \right) dx^i dx^j \right). \quad (2)$$

By substituting the perturbed metric in Eq. (2) into the Einstein’s field equation and simplifying, we derive the equation of motion for second-order GWs induced by first-order scalar perturbation $\phi^{(1)}$ during the radiation-dominated (RD) era

$$h_{lm}^{(2)''} + 2\mathcal{H}h_{lm}^{(2)'} - \Delta h_{lm}^{(2)} = -8\Lambda_{lm}^{rs} \phi^{(1)} \partial_r \partial_s \phi^{(1)}, \quad (3)$$

where $\Lambda_{rs}^{lm} = \mathcal{T}_r^l \mathcal{T}_s^m - \frac{1}{2} \mathcal{T}_{rs} \mathcal{T}^{lm}$ is the transverse and traceless decomposition operator, and \mathcal{T}_r^l is defined as $\mathcal{T}_r^l = \delta_r^l - \partial^l \Delta^{-1} \partial_r$ [43].

Similarly, for fourth-order GWs $h_{ij}^{(4)}$ induced by second-order scalar perturbation $\phi^{(2)}$, we set $\phi = \frac{1}{2} \phi^{(2)}$, $h_{ij} = \frac{1}{4!} h_{ij}^{(4)}$, and $\psi = V_i = 0$. The perturbed metric in Eq. (1) can be expressed as

$$ds^2 = a^2 \left(-(1 + \phi^{(2)}) d\eta^2 + \left(\delta_{ij} + \frac{1}{4!} h_{ij}^{(4)} \right) dx^i dx^j \right). \quad (4)$$

Interestingly, comparing the perturbed metrics between Eq. (2) and Eq. (4) reveals that their forms are entirely identical. The transformation between these two perturbed metrics can be achieved through a straightforward variable replacement: $\phi^{(1)} \rightarrow \frac{1}{2} \phi^{(2)}$ and $\frac{1}{2} h_{ij}^{(2)} \rightarrow \frac{1}{4!} h_{ij}^{(4)}$. By applying the variable replacement to Eq. (3), we obtain

$$h_{lm}^{(4)''} + 2\mathcal{H}h_{lm}^{(4)'} - \Delta h_{lm}^{(4)} = -48\Lambda_{lm}^{rs} \phi^{(2)} \partial_r \partial_s \phi^{(2)}. \quad (5)$$

This equation is consistent with the direct computational outcome from higher-order CP theory. Consequently, we reach a crucial conclusion: the equation of motion for second-order GWs induced by first-order scalar perturbation $\phi^{(1)}$ shares the same form as that for fourth-order GWs induced by second-order scalar perturbation $\phi^{(2)}$, except for the Taylor expansion coefficients. Since the perturbed metrics in Eq. (2) and Eq. (4) have exactly the same form, it is not surprising that they yield perturbation equations with identical forms. This conclusion can be extended to arbitrary higher-order induced GWs. For example, we express the equation of motion for n -th order GWs sourced by the product of lower-order perturbations $\phi^{(n-m)}$ and $\psi^{(m)}$ in a formal form as

$$h_{lm}^{(n)''} + 2\mathcal{H}h_{lm}^{(n)'} - \Delta h_{lm}^{(n)} = -n! \Lambda_{lm}^{rs} \times \mathcal{S}_{rs}^n \left(\phi^{(n-m)}, \psi^{(m)} \right), \quad (6)$$

where $\mathcal{S}_{rs}^n \left(\phi^{(n-m)}, \psi^{(m)} \right)$ represents the source term composed of the product of $\phi^{(n-m)}$ and $\psi^{(m)}$. The dynamical term on the left-hand side of the equation is fully determined and remains independent of the order of GWs being solved. Aside from the Taylor expansion coefficients, the source terms on the right-hand side of the equation depend only on the types of lower-order perturbations that constitute the source terms, and not on the order of these perturbations.

The above discussion inspires us to directly obtain the equations of motion for higher-order induced GWs by replacing variables between perturbations of the same type but different orders. Building upon this insight, we will present the vertex approach for

studying higher-order GWs, streamlining and enhancing the efficiency of the research on higher-order effects.

Vertex of induced GWs.—In Newtonian gauge, the equations of motion for the four types of CPs in Eq. (1) during the RD era can be expressed as [96, 97]

$$\begin{aligned} \psi^{(n)''} + 3\mathcal{H}\psi^{(n)'} - \frac{5}{6}\Delta\psi^{(n)} + \mathcal{H}\phi^{(n)'} + \frac{1}{2}\Delta\phi^{(n)} \\ = -\frac{n!}{4}\mathcal{T}^{rs}\mathcal{S}_{rs}^{(n)}, \end{aligned} \quad (7)$$

$$\begin{aligned} \psi^{(n)} - \phi^{(n)} = -n!\Delta^{-1}(\partial^r\Delta^{-1}\partial^s \\ - \frac{1}{2}\mathcal{T}^{rs})\mathcal{S}_{rs}^{(n)}, \end{aligned} \quad (8)$$

$$V_l^{(n)'} + 2\mathcal{H}V_l^{(n)} = 2n!\Delta^{-1}\mathcal{T}_l^r\partial^s\mathcal{S}_{rs}^{(n)}, \quad (9)$$

$$h_{lm}^{(n)''} + 2\mathcal{H}h_{lm}^{(n)'} - \Delta h_{lm}^{(n)} = -2n!\Lambda_{lm}^{rs}\mathcal{S}_{rs}^{(n)}, \quad (10)$$

where $\mathcal{H} = a'/a = 1/\eta$ is the conformal Hubble parameter. Superscript n represents the order of CPs, and $\mathcal{S}_{rs}^{(n)}$ denotes the source term composed of lower-order CPs. In Eq. (7)–Eq. (10), we have assumed $p^{(n)} = \frac{1}{3}\rho^{(n)}$, where $p^{(n)}$ and $\rho^{(n)}$ are n -th order pressure and density perturbations, respectively. The n -th order CP equation is determined by three components: (1) the dynamical term on the left-hand side of the equation; (2) the decomposition operators associated with the four kinds of n -th order perturbations: \mathcal{T}^{rs} , $\Delta^{-1}(\partial^r\Delta^{-1}\partial^s - \frac{1}{2}\mathcal{T}^{rs})$, $\Delta^{-1}\mathcal{T}_l^r\partial^s$, and Λ_{rs}^{lm} ; and (3) the source term on the right-hand side composed of lower-order perturbations. Eq. (7)–Eq. (10) can be studied in terms of vertex diagrams. We summarize the physical information contained in the n -branch vertex diagrams as follows:

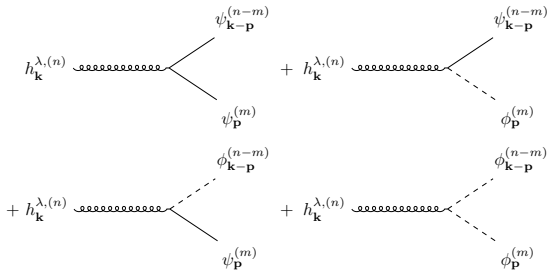


FIG. 1: The 2-branch vertex diagram of higher-order gravitational waves induced by the product of two first-order scalar perturbations. The dashed line, solid line, and spring-like line represent scalar perturbation ϕ , scalar perturbation ψ , and tensor perturbation h_{ij} , respectively.

a, Green's function and decomposed operators: the curve on the left side of the vertex diagram

in Fig. 1 corresponds to the n -th order CP that needs to be solved. The dynamical terms and decomposition operators in n -th order CP equations depend exclusively on the type of perturbation, resulting in the same Green's function for perturbations of the same type. Once the curve on the left side of the vertex diagram is determined, the Green's function of the perturbation equation and the corresponding decomposition operator are fully specified. The formal expressions for the higher-order induced GWs corresponding to the four vertex graphs in Fig. 1 are

$$\begin{aligned} h_{\mathbf{k},ss}^{\lambda,(n)}(\eta) = - \sum_{A=\psi,\phi} \frac{2n!}{k} \int_0^\eta d\tilde{\eta} \sin(k\eta - k\tilde{\eta}) \frac{\tilde{\eta}}{\eta} \\ \times \varepsilon^{\lambda,ij}(\mathbf{k})\mathcal{S}_{ij,ss}^{(n)}(\mathbf{k}, \tilde{\eta}), \end{aligned} \quad (11)$$

where $\mathcal{S}_{ij,ss}^{(n)}(\mathbf{k}, \tilde{\eta})$ is the n -th order source term. We have used the symbol $h_{\mathbf{k},ss}^{\lambda,(n)}$ to represent the higher-order SIGWs sourced by lower-order scalar perturbations $s = \psi, \phi$ [98]. The formal expressions of $\phi_{\mathbf{k}}^{(n)}$, $\psi_{\mathbf{k}}^{(n)}$, and $V_{\mathbf{k}}^{\lambda,(n)}$ can be found in Refs. [99, 100].

b, Source term: the branches on the right side of the vertex diagram correspond to the source terms formed by lower-order CPs. As mentioned in the previous section, higher-order source terms can be constructed by replacing variables in lower-order source terms. When the number and types of branches on the right side are completely determined, the form of the source terms is also fully determined. The explicit expressions for the four kinds of source terms corresponding to Fig. 1 are as follows

$$\begin{aligned} \mathcal{S}_{ij,\psi\psi}^{(n)}(\mathbf{k}, \eta) = \frac{1}{m!(n-m)!} \int \frac{d^3p}{(2\pi)^{3/2}} p_i p_j \\ \left(\frac{2}{\mathcal{H}^2} \psi_{\mathbf{k}-\mathbf{p}}^{(n-m)'} \psi_{\mathbf{p}}^{(m)'} - 2\psi_{\mathbf{k}-\mathbf{p}}^{(n-m)} \psi_{\mathbf{p}}^{(m)} \right), \end{aligned} \quad (12)$$

$$\begin{aligned} \mathcal{S}_{ij,\psi\phi}^{(n)}(\mathbf{k}, \eta) = \frac{1}{m!(n-m)!} \int \frac{d^3p}{(2\pi)^{3/2}} p_i p_j \\ \times \frac{2}{\mathcal{H}} \psi_{\mathbf{k}-\mathbf{p}}^{(n-m)'} \phi_{\mathbf{p}}^{(m)}, \end{aligned} \quad (13)$$

$$\begin{aligned} \mathcal{S}_{ij,\phi\psi}^{(n)}(\mathbf{k}, \eta) = \frac{1}{m!(n-m)!} \int \frac{d^3p}{(2\pi)^{3/2}} p_i p_j \\ \times \frac{2}{\mathcal{H}} \psi_{\mathbf{k}-\mathbf{p}}^{(m)'} \phi_{\mathbf{p}}^{(n-m)}, \end{aligned} \quad (14)$$

$$\begin{aligned} \mathcal{S}_{ij,\phi\phi}^{(n)}(\mathbf{k}, \eta) = \frac{1}{m!(n-m)!} \int \frac{d^3p}{(2\pi)^{3/2}} p_i p_j \\ \times 4\phi_{\mathbf{k}-\mathbf{p}}^{(n-m)} \phi_{\mathbf{p}}^{(m)}. \end{aligned} \quad (15)$$

The source terms in Eq. (12)–Eq. (15) have been simplified using the property of the transverse and traceless operator $\Lambda_{ij}^{rs} \partial_i \phi \partial_j \phi = -\Lambda_{ij}^{rs} \phi \partial_i \partial_j \phi$.

c, Momentum integrals: in the case of a vertex diagram with n branches on the right-hand side, the associated source term is formed by multiplying n lower-order perturbations. Consequently, the expression for an n -branch vertex diagram will include $n - 1$ momentum integrals.

In Fig. 1 and Eq. (12)–Eq. (15), we present the 2-branch vertex diagrams along with the corresponding source terms. This result can also be extended to other types of source terms and multi-branch vertex diagrams. Since the Green’s function, decomposition operator, and momentum integral are fully determined by the vertex diagram, for different types of multi-branch vertex diagrams, we only need to calculate the source term corresponding to the vertex diagram. To derive the source terms related to multi-branch vertices, we need to investigate the n -th order perturbations of the Einstein’s field equation using the metric perturbation in Eq. (1). In the supplementary material, we derive the explicit expressions for n -th order perturbations of the Einstein’s field equation $G_{\mu\nu} = \kappa T_{\mu\nu}$ during the RD era in Newtonian gauge and present the source terms associated with all types of 2-branch vertex diagrams.

Tree diagrams of induced GWs.—As shown in Eq. (3) and Eq. (5), while the second-order GWs $h_{lm}^{(2)}$ and the fourth-order GWs $h_{lm}^{(4)}$ have identical equations of motion, their explicit expressions vary due to the differences in the first-order scalar perturbation $\phi^{(1)}$ and the second-order scalar perturbation $\phi^{(2)}$ in the source terms. The vertex rules associated with the vertex diagram in Fig. 1 describe the relationship between n -th order induced GWs and lower-order perturbations. However, it does not directly provide the explicit expression for n -th order induced GWs. A single vertex diagram is insufficient to fully describe higher-order induced GWs.

In conventional approaches, obtaining the explicit expression for n -th order induced GWs involves solving the CP equations iteratively, starting from first-order perturbations. In the vertex approach, we allow the branches on the right side of the vertex diagram to bifurcate into new vertices, resembling the growth of a tree, until all emerging branches correspond exclusively to first-order perturbations. As illustrated in Fig. 2, since the analytical solutions of the first-order perturbations are known, the ‘fully grown’ tree diagram allows us to systematically derive the expression for higher-order induced GWs using the vertex approach.

In previous studies, similar vertex diagrams were typically used as conceptual illustrations without significant practical value. However, as our research re-

veals, both vertex diagrams and the resulting tree diagrams carry profound physical implications. The vertex approach significantly streamlines the calculation of higher-order induced GWs. To compute the n -th order induced GWs, one needs only to generate all possible inequivalent tree diagrams and write down the corresponding expressions for each tree diagram according to the vertex rules. By summing up these tree diagrams, we obtain the explicit expression for the n -th order induced GWs.

1PR diagrams of induced GWs.—Calculating the two-point correlation function of GWs yields their energy density spectrum, a key observable in SGWB experiments. Within the vertex approach, the explicit expression for induced GWs can be directly derived from tree diagrams. The two-point correlation function of induced GWs corresponds to loop diagrams formed by connecting two tree diagrams. Different connection patterns between these two tree diagrams lead to distinct types of loop diagrams, which align with the Wick expansion of the multi-point correlation function of primordial perturbations [84]. We concentrate on the simplest loop diagram structure: 1PR diagrams in third-order induced GWs. In the calculation of two-loop diagrams of SIGWs, 1PR diagrams have no impact on the two-point correlation function. As shown in Fig. 3a, the two-point correlation function of third-order SIGWs associated with the 1PR diagram can be expressed as

$$\begin{aligned} \delta(\mathbf{k} + \mathbf{k}') & \frac{2\pi^2}{k^3} \langle h_{\mathbf{k},\phi\psi\phi\phi}^{\lambda,(3)} h_{\mathbf{k}',\phi\psi\phi\phi}^{\lambda',(3)} \rangle \\ & = \langle h_{\mathbf{k},\phi\psi\phi\phi}^{\lambda,(3)} \phi_{\mathbf{k}'}^{(1)} \rangle \frac{1}{\mathcal{P}_\zeta(k) T_\phi^2(k'\eta)} \langle \phi_{\mathbf{k}}^{(1)} h_{\mathbf{k}',\phi\psi\phi\phi}^{\lambda',(3)} \rangle, \end{aligned} \quad (16)$$

where

$$\begin{aligned} \langle h_{\mathbf{k},\phi\psi\phi\phi}^{\lambda,(3)} \phi_{\mathbf{k}'}^{(1)} \rangle & = \int \frac{d^3p}{(2\pi)^{3/2}} \int \frac{d^3q}{(2\pi)^{3/2}} \varepsilon^{\lambda,lm}(\mathbf{k}) p_l p_m \\ & \frac{16}{81} I_{\phi\psi\phi\phi}^{(3)}(|\mathbf{k} - \mathbf{p}|, |\mathbf{p} - \mathbf{q}|, |\mathbf{q}|, \eta) T_\phi(k'\eta) \\ & \langle \zeta_{\mathbf{k}-\mathbf{p}} \zeta_{\mathbf{p}-\mathbf{q}} \rangle \langle \zeta_{\mathbf{q}} \zeta_{\mathbf{k}'} \rangle. \end{aligned} \quad (17)$$

In Eq. (16) and Eq. (17), $\zeta_{\mathbf{k}}$ represents the primordial curvature perturbation, and $\mathcal{P}_\zeta(k)$ is the corresponding primordial power spectrum. $I_{\phi\psi\phi\phi}^{(3)}$ is the third-order kernel function [86]. $T_\phi(k\eta)$ is the transfer function of first-order scalar perturbation [100]. Here, the 1PR diagram of third-order SIGWs is decomposed into the product of two one-particle irreducible (1PI) diagrams. Therefore, we only need to consider the two-point function $\langle h_{\mathbf{k}',\phi\psi\phi\phi}^{\lambda,(3)} \phi_{\mathbf{k}}^{(1)} \rangle$. In

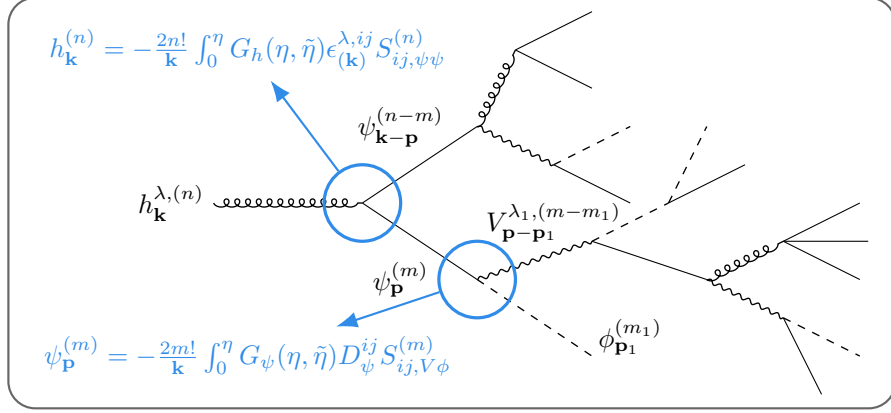


FIG. 2: The tree diagram of induced GWs. $G_h(\eta, \bar{\eta})$ and $G_\psi(\eta, \bar{\eta})$ represent the Green's functions of tensor perturbation h_{ij} and scalar perturbation ψ , respectively. The first vertex illustrates the relationship between the n -th order induced GWs $h_{\mathbf{k}}^{(n)}$ and the lower-order perturbations $\psi_{\mathbf{k}-\mathbf{p}}^{(n-m)}$ and $\psi_{\mathbf{p}}^{(m)}$ in the corresponding source term. The second vertex shows the relationship between the perturbation $\psi_{\mathbf{p}}^{(m)}$ and the lower-order perturbations $V_{\mathbf{p}-\mathbf{p}_1}^{\lambda_1, (m-m_1)}$ and $\phi_{\mathbf{p}_1}^{(m_1)}$. Following this pattern, we can use vertex rules and tree diagrams to express the n -th order induced GWs entirely in terms of first-order perturbations.

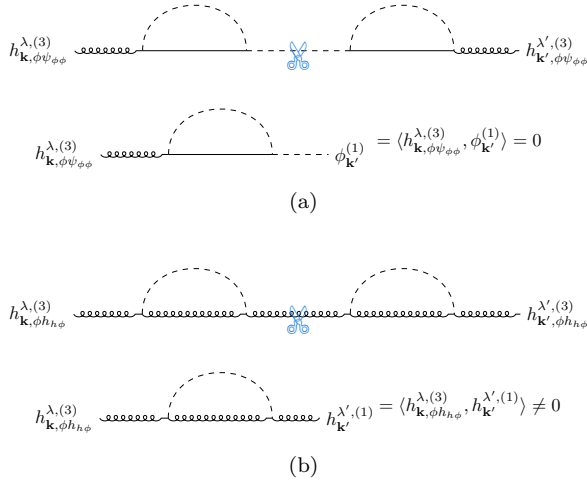


FIG. 3: The 1PR diagrams resulting from the contraction of two-branch tree diagrams of third-order induced GWs.

Eq. (17), the momentum integral can be calculated in a spherical coordinate system with \mathbf{k} as the z -axis. In this case, the contraction of the polarization tensor $\varepsilon^{\lambda, lm}(\mathbf{k})$ with momenta p_l and p_m can be expressed as [12]

$$\varepsilon^{\lambda, lm}(\mathbf{k})p_l p_m = \frac{p^2}{\sqrt{2}} \sin^2 \theta_p \times \begin{cases} \cos 2\phi_p, & \lambda = + \\ \sin 2\phi_p, & \lambda = \times \end{cases} \quad (18)$$

Notably, the kernel function $I_{\phi\psi\phi\phi}^{(3)}$ in Eq. (17) relies solely on the relative positions of \mathbf{k} , \mathbf{p} , and \mathbf{q} , completely independent of the overall azimuth angle ϕ_p . Integrating over ϕ_p yields $\int_0^{2\pi} \varepsilon^{\lambda, lm}(\mathbf{k})p_l p_m d\phi_p = 0$. Consequently, the two-point correlation function $\langle h_{\mathbf{k}', \phi\psi\phi\phi}^{\lambda, (3)} \phi_{\mathbf{k}}^{(1)} \rangle = 0$, and the 1PR diagrams of third-order SIGWs do not contribute to the energy density spectrum. This conclusion can be generalized to arbitrary higher-order SIGWs with different kinds of source terms. However, the above results are not applicable to T-SIGWs.

T-SIGWs arise from primordial tensor and scalar perturbations with large amplitudes on small scales [93]. For example, as shown in Fig. 3b, the 1PR diagram for third-order T-SIGWs can be decomposed into the product of two 1PI diagrams. In this case, the polarized tensor $\varepsilon^{\lambda, lm}(\mathbf{k})$ in the two-point correlation function $\langle h_{\mathbf{k}}^{\lambda, (3)} h_{\mathbf{k}'}^{\lambda_1, (1)} \rangle$ will contract with other polarized tensors [95]. The corresponding two-point function can be written as

$$\begin{aligned} \delta(\mathbf{k} + \mathbf{k}') \frac{2\pi^2}{k^3} \langle h_{\mathbf{k}, \phi h \phi}^{\lambda, (3)} h_{\mathbf{k}', \phi h \phi}^{\lambda', (3)} \rangle \\ = \langle h_{\mathbf{k}, \phi h \phi}^{\lambda, (3)} h_{\mathbf{k}'}^{\lambda_1, (1)} \rangle \frac{\delta_{\lambda_1 \lambda'_1}}{\mathcal{P}_h(k') T_h^2(k'\eta)} \langle h_{\mathbf{k}}^{\lambda'_1, (1)} h_{\mathbf{k}', \phi h \phi}^{\lambda', (3)} \rangle, \end{aligned} \quad (19)$$

where $\mathcal{P}_h(k')$ and $T_h^2(k'\eta)$ represent the primordial power spectrum and the first-order transfer function of tensor perturbation, respectively. The explicit expressions of $h_{\mathbf{k}, sh_{sh}}^{\lambda, (3)}$ ($s = \phi, \psi$) are given in the supplementary material. As shown in Fig. 4, in

the case of the log-normal primordial power spectra: $A_\zeta (2\pi\sigma_\zeta^2)^{-1/2} \exp(-\ln^2(k/k_*)/(2\sigma_\zeta^2))$ and $A_h (2\pi\sigma_h^2)^{-1/2} \exp(-\ln^2(k/k_*)/(2\sigma_h^2))$, the 1PR diagram of $h_{\mathbf{k},sh_s h}^{\lambda,(3)}$ will have a non-zero impact on the total energy density spectrum of induced GWs.

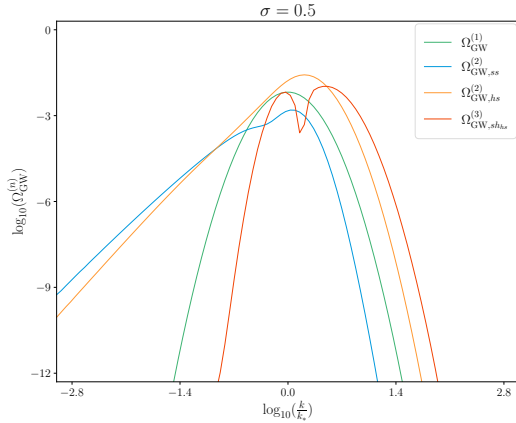


FIG. 4: The green line, blue line, orange line, and red line correspond to the energy density spectra of first-order GWs $h_{\mathbf{k}}^{\lambda,(1)}$, second-order SIGWs $h_{\mathbf{k},ss}^{\lambda,(2)}$, second-order T-SIGWs $h_{\mathbf{k},sh}^{\lambda,(2)}$, and 1PR diagrams of third-order T-SIGWs $h_{\mathbf{k},sh_s h}^{\lambda,(3)}$, respectively. The symbols $s = \phi, \psi$ and h represent scalar perturbations and tensor perturbation, respectively. We set $A_\zeta = A_h = 0.1$ and $\sigma_\zeta = \sigma_h = 0.5$.

It should be noted that in higher-order CP theory, the curves in tree and loop diagrams also encode the order of CPs. When decomposing a 1PR diagram into multiple 1PI diagrams, it is crucial to consider the order of the perturbations associated with the 'cut' curves. As shown in Fig. 5, the 1PR diagram cannot be simply expressed as $\langle h_{\mathbf{k}}^{\lambda,(n)} h_{\mathbf{k}'}^{\lambda',(n')} \rangle \sim \langle h_{\mathbf{k}}^{\lambda,(n)} h_{\mathbf{k}'}^{\lambda',(1)} \rangle^3$. The correct decomposition obtained through direct calculation is

$$\langle h_{\mathbf{k}}^{\lambda,(n)} h_{\mathbf{k}'}^{\lambda',(n')} \rangle \sim \langle h_{\mathbf{k}}^{\lambda,(n)} h_{\mathbf{k}'}^{\lambda_1,(m_1)} \rangle \langle h_{\mathbf{k}}^{\lambda_1,(m_1)} h_{\mathbf{k}'}^{\lambda_2,(m_2)} \rangle \langle h_{\mathbf{k}}^{\lambda_2,(m_2)} h_{\mathbf{k}'}^{\lambda',(n')} \rangle. \quad (20)$$

As shown in Table. I, the physical implications of tree diagrams and loop diagrams in classical higher-order CPs are different from those of Feynman diagrams in quantum field theory (QFT). All the calculation techniques for tree diagrams and loop diagrams involved here must be derived or proven from basic definitions.

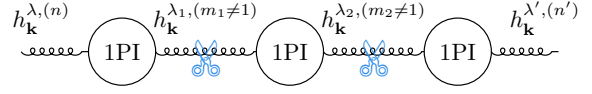


FIG. 5: In higher-order cosmological perturbation theory, the decomposition of 1PR diagrams requires consideration of the order of perturbations.

	QFT	Classical CPs
Origin	Dyson series	CP equations
Tree diagram	Lowest-order contribution	Explicit expression of CPs
Loop diagram	Higher-order correction	Two-point function
External lines	Particles	CPs

TABLE I: The distinction between Feynman diagrams in QFT and diagrams in classical CP theory.

Conclusion.—Over the past few years, considerable interest has focused on large primordial perturbations at small scales. The large primordial perturbations play a pivotal role in areas such as PBHs and induced GWs. In this scenario, the influence of higher-order CPs on small-scale cosmological observations is non-negligible. If higher-order CPs are not systematically calculated or rigorously estimated, and only lower-order perturbations are considered, the cosmological parameters derived from current observations, such as the small-scale primordial power spectrum, will significantly deviate from their true values. Systematically investigating the effects of higher-order CPs during various dominant epochs and in different gauges on small-scale cosmological observations is undoubtedly a crucial and fundamental challenge.

Traditional CP theory requires order-by-order derivation and solution of higher-order perturbation equations to obtain the formal solutions of higher-order CPs. The complexity and tediousness of these calculations make it difficult to apply conventional methods to the study of arbitrary higher-order CPs. We proposed the vertex approach for directly constructing higher-order CPs from the equations of motion of lower-order CPs. Utilizing tree diagrams and vertex rules, one can derive the specific expressions for higher-order CPs. In this Letter, we focus on the higher-order induced GWs during the RD era in Newtonian gauge, the theoretical framework of vertex approach can be extended to various types of CPs, different dominant epochs of the universe, and different gauges.

In investigating induced GWs, solving higher-

order CPs is only part of the task. We also need to compute two-point correlation functions to derive the energy density spectrum, represented by loop diagrams connecting different tree diagrams. Using vertex rules, we can derive expressions for these loop diagrams. However, due to the variety and complexity of loop diagrams, merely providing explicit expressions is insufficient. We also need to classify loop diagrams by structure and simplify calculations to improve efficiency. The relevant research might be presented in the future.

The authors want to thank Dr. Fei-Yu Chen and Dr. Quan-feng Wu for useful discussions. This work has been funded by the National Nature Science Foundation of China (NSFC) under grant No. 12075249, No. 11690022, No. 12475075, No. 11935009, and No. 12375052. And the Key Research Program of the Chinese Academy of Sciences under Grant No. XDPB15.

-
- [1] N. Bartolo, E. Komatsu, S. Matarrese, and A. Riotto, *Phys. Rept.* **402**, 103 (2004), [arXiv:astro-ph/0406398](#).
- [2] D. H. Lyth and A. Riotto, *Phys. Rept.* **314**, 1 (1999), [arXiv:hep-ph/9807278](#).
- [3] M. Novello and S. E. P. Bergliaffa, *Phys. Rept.* **463**, 127 (2008), [arXiv:0802.1634 \[astro-ph\]](#).
- [4] N. Aghanim *et al.* (Planck), *Astron. Astrophys.* **641**, A6 (2020), [Erratum: *Astron. Astrophys.* 652, C4 (2021)], [arXiv:1807.06209 \[astro-ph.CO\]](#).
- [5] N. Aghanim *et al.* (Planck), *Astron. Astrophys.* **641**, A1 (2020), [arXiv:1807.06205 \[astro-ph.CO\]](#).
- [6] B. Carr, F. Kuhnel, and M. Sandstad, *Phys. Rev. D* **94**, 083504 (2016), [arXiv:1607.06077 \[astro-ph.CO\]](#).
- [7] B. Carr, K. Kohri, Y. Sendouda, and J. Yokoyama, *Rept. Prog. Phys.* **84**, 116902 (2021), [arXiv:2002.12778 \[astro-ph.CO\]](#).
- [8] G. Agazie *et al.* (NANOGrav), *Astrophys. J. Lett.* **951**, L8 (2023), [arXiv:2306.16213 \[astro-ph.HE\]](#).
- [9] D. J. Reardon *et al.*, *Astrophys. J. Lett.* **951**, L6 (2023), [arXiv:2306.16215 \[astro-ph.HE\]](#).
- [10] J. Antoniadis *et al.* (EPTA), *Astron. Astrophys.* **678**, A50 (2023), [arXiv:2306.16214 \[astro-ph.HE\]](#).
- [11] H. Xu *et al.*, *Res. Astron. Astrophys.* **23**, 075024 (2023), [arXiv:2306.16216 \[astro-ph.HE\]](#).
- [12] G. Domènech, *Universe* **7**, 398 (2021), [arXiv:2109.01398 \[gr-qc\]](#).
- [13] A. Afzal *et al.* (NANOGrav), *Astrophys. J. Lett.* **951**, L11 (2023), [arXiv:2306.16219 \[astro-ph.HE\]](#).
- [14] S. Wang, Z.-C. Zhao, J.-P. Li, and Q.-H. Zhu, (2023), [arXiv:2307.00572 \[astro-ph.CO\]](#).
- [15] S. Choudhury, K. Dey, A. Karde, S. Panda, and M. Sami, (2023), [arXiv:2310.11034 \[astro-ph.CO\]](#).
- [16] J. Ellis, M. Fairbairn, G. Franciolini, G. Hütsi, A. Iovino, M. Lewicki, M. Raidal, J. Urrutia, V. Vaskonen, and H. Veermäe, *Phys. Rev. D* **109**, 023522 (2024), [arXiv:2308.08546 \[astro-ph.CO\]](#).
- [17] S. Balaji, G. Domènech, and G. Franciolini, *JCAP* **10**, 041 (2023), [arXiv:2307.08552 \[gr-qc\]](#).
- [18] Z.-Q. You, Z. Yi, and Y. Wu, (2023), [arXiv:2307.04419 \[gr-qc\]](#).
- [19] S. Mollerach, D. Harari, and S. Matarrese, *Phys. Rev. D* **69**, 063002 (2004), [arXiv:astro-ph/0310711](#).
- [20] K. N. Ananda, C. Clarkson, and D. Wands, *Phys. Rev. D* **75**, 123518 (2007), [arXiv:gr-qc/0612013](#).
- [21] B. Osano, C. Pitrou, P. Dunsby, J.-P. Uzan, and C. Clarkson, *JCAP* **04**, 003 (2007), [arXiv:gr-qc/0612108](#).
- [22] D. Baumann, P. J. Steinhardt, K. Takahashi, and K. Ichiki, *Phys. Rev. D* **76**, 084019 (2007), [arXiv:hep-th/0703290](#).
- [23] S. Wang, T. Terada, and K. Kohri, *Phys. Rev. D* **99**, 103531 (2019), [Erratum: *Phys. Rev. D* 101, 069901 (2020)], [arXiv:1903.05924 \[astro-ph.CO\]](#).
- [24] C. T. Byrnes, P. S. Cole, and S. P. Patil, *JCAP* **06**, 028 (2019), [arXiv:1811.11158 \[astro-ph.CO\]](#).
- [25] K. Inomata, M. Kawasaki, K. Mukaida, T. Terada, and T. T. Yanagida, *Phys. Rev. D* **101**, 123533 (2020), [arXiv:2003.10455 \[astro-ph.CO\]](#).
- [26] G. Ballesteros, J. Rey, M. Taoso, and A. Urbano, *JCAP* **07**, 025 (2020), [arXiv:2001.08220 \[astro-ph.CO\]](#).
- [27] J. Lin, Q. Gao, Y. Gong, Y. Lu, C. Zhang, and F. Zhang, *Phys. Rev. D* **101**, 103515 (2020), [arXiv:2001.05909 \[gr-qc\]](#).
- [28] Z.-C. Chen, C. Yuan, and Q.-G. Huang, *Phys. Rev. Lett.* **124**, 251101 (2020), [arXiv:1910.12239 \[astro-ph.CO\]](#).
- [29] R.-G. Cai, S. Pi, S.-J. Wang, and X.-Y. Yang, *JCAP* **10**, 059 (2019), [arXiv:1907.06372 \[astro-ph.CO\]](#).
- [30] Y.-F. Cai, C. Chen, X. Tong, D.-G. Wang, and S.-F. Yan, *Phys. Rev. D* **100**, 043518 (2019), [arXiv:1902.08187 \[astro-ph.CO\]](#).
- [31] K. Ando, K. Inomata, and M. Kawasaki, *Phys. Rev. D* **97**, 103528 (2018), [arXiv:1802.06393 \[astro-ph.CO\]](#).
- [32] H. Di and Y. Gong, *JCAP* **07**, 007 (2018), [arXiv:1707.09578 \[astro-ph.CO\]](#).
- [33] Q. Gao, *Sci. China Phys. Mech. Astron.* **64**, 280411 (2021), [arXiv:2102.07369 \[gr-qc\]](#).
- [34] Z. Chang, Y.-T. Kuang, X. Zhang, and J.-Z. Zhou, (2022), [arXiv:2211.11948 \[astro-ph.CO\]](#).
- [35] Z. Zhou, J. Jiang, Y.-F. Cai, M. Sasaki, and S. Pi, *Phys. Rev. D* **102**, 103527 (2020), [arXiv:2010.03537 \[astro-ph.CO\]](#).
- [36] R.-G. Cai, C. Chen, and C. Fu, *Phys. Rev. D* **104**, 083537 (2021), [arXiv:2108.03422 \[astro-ph.CO\]](#).
- [37] G. Domènech and M. Sasaki, *Class. Quant. Grav.* **41**, 143001 (2024), [arXiv:2401.07615 \[gr-qc\]](#).
- [38] J.-C. Hwang, D. Jeong, and H. Noh, *Astrophys. J.* **842**, 46 (2017), [arXiv:1704.03500 \[astro-ph.CO\]](#).
- [39] C. Yuan, Z.-C. Chen, and Q.-G. Huang, *Phys. Rev. D* **101**, 063018 (2020), [arXiv:1912.00885 \[astro-ph.CO\]](#).
- [40] K. Inomata and T. Terada, *Phys. Rev. D* **101**,

- 023523 (2020), arXiv:1912.00785 [gr-qc].
- [41] V. De Luca, G. Franciolini, A. Kehagias, and A. Riotto, *JCAP* **03**, 014 (2020), arXiv:1911.09689 [gr-qc].
- [42] G. Domènech and M. Sasaki, *Phys. Rev. D* **103**, 063531 (2021), arXiv:2012.14016 [gr-qc].
- [43] Z. Chang, S. Wang, and Q.-H. Zhu, *Chin. Phys. C* **45**, 095101 (2021), arXiv:2009.11025 [astro-ph.CO].
- [44] A. Ali, Y. Gong, and Y. Lu, *Phys. Rev. D* **103**, 043516 (2021), arXiv:2009.11081 [gr-qc].
- [45] Y. Lu, A. Ali, Y. Gong, J. Lin, and F. Zhang, *Phys. Rev. D* **102**, 083503 (2020), arXiv:2006.03450 [gr-qc].
- [46] K. Tomikawa and T. Kobayashi, *Phys. Rev. D* **101**, 083529 (2020), arXiv:1910.01880 [gr-qc].
- [47] J. Gurian, D. Jeong, J.-c. Hwang, and H. Noh, *Phys. Rev. D* **104**, 083534 (2021), arXiv:2104.03330 [astro-ph.CO].
- [48] C. Uggla and J. Wainwright, *Class. Quant. Grav.* **36**, 035004 (2019), arXiv:1801.04300 [gr-qc].
- [49] A. Ali, Y.-P. Hu, M. Sabir, and T. Sui, *Sci. China Phys. Mech. Astron.* **66**, 290411 (2023), arXiv:2308.04713 [gr-qc].
- [50] R.-g. Cai, S. Pi, and M. Sasaki, *Phys. Rev. Lett.* **122**, 201101 (2019), arXiv:1810.11000 [astro-ph.CO].
- [51] V. Atal and G. Domènech, *JCAP* **06**, 001 (2021), arXiv:2103.01056 [astro-ph.CO].
- [52] F. Zhang, Y. Gong, J. Lin, Y. Lu, and Z. Yi, *JCAP* **04**, 045 (2021), arXiv:2012.06960 [astro-ph.CO].
- [53] C. Yuan and Q.-G. Huang, *Phys. Lett. B* **821**, 136606 (2021), arXiv:2007.10686 [astro-ph.CO].
- [54] M. W. Davies, P. Carrilho, and D. J. Mulryne, *JCAP* **06**, 019 (2022), arXiv:2110.08189 [astro-ph.CO].
- [55] K. Reza zadeh, Z. Teimoori, S. Karimi, and K. Karami, *Eur. Phys. J. C* **82**, 758 (2022), arXiv:2110.01482 [gr-qc].
- [56] J. Kristiano and J. Yokoyama, *Phys. Rev. Lett.* **128**, 061301 (2022), arXiv:2104.01953 [hep-th].
- [57] N. Bartolo, V. Domcke, D. G. Figueroa, J. García-Bellido, M. Peloso, M. Pieroni, A. Ricciardone, M. Sakellariadou, L. Sorbo, and G. Tasinato, *JCAP* **11**, 034 (2018), arXiv:1806.02819 [astro-ph.CO].
- [58] P. Adshead, K. D. Lozanov, and Z. J. Weiner, *JCAP* **10**, 080 (2021), arXiv:2105.01659 [astro-ph.CO].
- [59] J.-P. Li, S. Wang, Z.-C. Zhao, and K. Kohri, *JCAP* **10**, 056 (2023), arXiv:2305.19950 [astro-ph.CO].
- [60] J.-P. Li, S. Wang, Z.-C. Zhao, and K. Kohri, (2023), arXiv:2309.07792 [astro-ph.CO].
- [61] S. Garcia-Saenz, L. Pinol, S. Renaux-Petel, and D. Werth, *JCAP* **03**, 057 (2023), arXiv:2207.14267 [astro-ph.CO].
- [62] J.-P. Li, S. Wang, Z.-C. Zhao, and K. Kohri, (2024), arXiv:2403.00238 [astro-ph.CO].
- [63] G. Perna, C. Testini, A. Ricciardone, and S. Matarrese, *JCAP* **05**, 086 (2024), arXiv:2403.06962 [astro-ph.CO].
- [64] K. Kohri and T. Terada, *Phys. Rev. D* **97**, 123532 (2018), arXiv:1804.08577 [gr-qc].
- [65] T. Papanikolaou, V. Vennin, and D. Langlois, *JCAP* **03**, 053 (2021), arXiv:2010.11573 [astro-ph.CO].
- [66] G. Domènech, S. Pi, and M. Sasaki, *JCAP* **08**, 017 (2020), arXiv:2005.12314 [gr-qc].
- [67] G. Domènech, *Int. J. Mod. Phys. D* **29**, 2050028 (2020), arXiv:1912.05583 [gr-qc].
- [68] K. Inomata, K. Kohri, T. Nakama, and T. Terada, *JCAP* **10**, 071 (2019), [Erratum: *JCAP* **08**, E01 (2023)], arXiv:1904.12878 [astro-ph.CO].
- [69] K. Inomata, K. Kohri, T. Nakama, and T. Terada, *Phys. Rev. D* **100**, 043532 (2019), [Erratum: *Phys. Rev. D* **108**, 049901 (2023)], arXiv:1904.12879 [astro-ph.CO].
- [70] H. Assadullahi and D. Wands, *Phys. Rev. D* **79**, 083511 (2009), arXiv:0901.0989 [astro-ph.CO].
- [71] L. T. Witkowski, G. Domènech, J. Fumagalli, and S. Renaux-Petel, *JCAP* **05**, 028 (2022), arXiv:2110.09480 [astro-ph.CO].
- [72] I. Dalianis and C. Kouvaris, *JCAP* **07**, 046 (2021), arXiv:2012.09255 [astro-ph.CO].
- [73] F. Hajkarim and J. Schaffner-Bielich, *Phys. Rev. D* **101**, 043522 (2020), arXiv:1910.12357 [hep-ph].
- [74] N. Bernal and F. Hajkarim, *Phys. Rev. D* **100**, 063502 (2019), arXiv:1905.10410 [astro-ph.CO].
- [75] S. Das, A. Maharana, and F. Muia, *Mon. Not. Roy. Astron. Soc.* **515**, 13 (2022), arXiv:2112.11486 [astro-ph.CO].
- [76] M. R. Haque, D. Maity, T. Paul, and L. Srimakumar, *Phys. Rev. D* **104**, 063513 (2021), arXiv:2105.09242 [astro-ph.CO].
- [77] G. Domènech, C. Lin, and M. Sasaki, *JCAP* **04**, 062 (2021), [Erratum: *JCAP* **11**, E01 (2021)], arXiv:2012.08151 [gr-qc].
- [78] G. Domènech, S. Passaglia, and S. Renaux-Petel, *JCAP* **03**, 023 (2022), arXiv:2112.10163 [astro-ph.CO].
- [79] L. Liu, Z.-C. Chen, and Q.-G. Huang, (2023), arXiv:2307.14911 [astro-ph.CO].
- [80] A. Mangilli, N. Bartolo, S. Matarrese, and A. Riotto, *Phys. Rev. D* **78**, 083517 (2008), arXiv:0805.3234 [astro-ph].
- [81] S. Saga, K. Ichiki, and N. Sugiyama, *Phys. Rev. D* **91**, 024030 (2015), arXiv:1412.1081 [astro-ph.CO].
- [82] X. Zhang, J.-Z. Zhou, and Z. Chang, *Eur. Phys. J. C* **82**, 781 (2022), arXiv:2208.12948 [astro-ph.CO].
- [83] C. Yuan, D.-S. Meng, and Q.-G. Huang, (2023), arXiv:2308.07155 [astro-ph.CO].
- [84] Z. Chang, Y.-T. Kuang, D. Wu, and J.-Z. Zhou, *JCAP* **2024**, 044 (2024), arXiv:2312.14409 [astro-ph.CO].
- [85] Z. Chang, Y.-T. Kuang, D. Wu, J.-Z. Zhou, and Q.-H. Zhu, *Phys. Rev. D* **109**, L041303 (2024), arXiv:2311.05102 [astro-ph.CO].
- [86] J.-Z. Zhou, X. Zhang, Q.-H. Zhu, and Z. Chang, *JCAP* **05**, 013 (2022), arXiv:2106.01641 [astro-ph.CO].
- [87] Z. Chang, Y.-T. Kuang, X. Zhang, and J.-Z. Zhou, *Chin. Phys. C* **47**, 055104 (2023), arXiv:2209.12404 [astro-ph.CO].
- [88] C. Yuan, Z.-C. Chen, and Q.-G. Huang, *Phys. Rev.*

- D **100**, 081301 (2019), [arXiv:1906.11549 \[astro-ph.CO\]](#).
- [89] S. Wang, Z.-C. Zhao, and Q.-H. Zhu, *Phys. Rev. Res.* **6**, 013207 (2024), [arXiv:2307.03095 \[astro-ph.CO\]](#).
- [90] K. A. Malik and D. Wands, *Phys. Rept.* **475**, 1 (2009), [arXiv:0809.4944 \[astro-ph\]](#).
- [91] C.-P. Ma and E. Bertschinger, *Astrophys. J.* **455**, 7 (1995), [arXiv:astro-ph/9506072](#).
- [92] C. Pitrou, X. Roy, and O. Umeh, *Class. Quant. Grav.* **30**, 165002 (2013), [arXiv:1302.6174 \[astro-ph.CO\]](#).
- [93] Z. Chang, X. Zhang, and J.-Z. Zhou, *Phys. Rev. D* **107**, 063510 (2023), [arXiv:2209.07693 \[astro-ph.CO\]](#).
- [94] P. Bari, N. Bartolo, G. Domènech, and S. Matarrese, *Phys. Rev. D* **109**, 023509 (2024), [arXiv:2307.05404 \[astro-ph.CO\]](#).
- [95] C. Chen, A. Ota, H.-Y. Zhu, and Y. Zhu, *Phys. Rev. D* **107**, 083518 (2023), [arXiv:2210.17176 \[astro-ph.CO\]](#).
- [96] T. H.-C. Lu, K. Ananda, C. Clarkson, and R. Maartens, *JCAP* **02**, 023 (2009), [arXiv:0812.1349 \[astro-ph\]](#).
- [97] Z. Chang, Y.-T. Kuang, X. Zhang, and J.-Z. Zhou, *Universe* **10**, 39 (2024), [arXiv:2211.11948 \[astro-ph.CO\]](#).
- [98] J. Ellis, *Comput. Phys. Commun.* **210**, 103 (2017), [arXiv:1601.05437 \[hep-ph\]](#).
- [99] Z. Chang, X. Zhang, and J.-Z. Zhou, *JCAP* **10**, 084 (2022), [arXiv:2207.01231 \[astro-ph.CO\]](#).
- [100] K. Inomata, *JCAP* **03**, 013 (2021), [arXiv:2008.12300 \[gr-qc\]](#).

Induced gravitational waves for arbitrary higher orders: vertex rules and loop diagrams in cosmological perturbation theory

Jing-Zhi Zhou, Yu-Ting Kuang, Di Wu, H. Lü, and Zhe Chang

Supplementary Material

HIGHER ORDER COSMOLOGICAL PERTURBATIONS

To determine the source terms associated with various vertex diagrams, we need to calculate the n -th order perturbations of the Einstein's field equation, considering only first-order scalar, vector, and tensor perturbations. The perturbation of the metric $g_{\mu\nu}$ in Friedmann-Lemaitre-Robertson-Walker background is given by

$$\begin{aligned} g_{\mu\nu}^{(0)} &= a^2 \eta_{\mu\nu} , \\ \delta g_{\mu\nu} &= a^2 h_{\mu\nu} - a^2 V_\nu n_\mu - a^2 V_\mu n_\nu - 2a^2 n_\mu n_\nu \phi - 2a^2 \psi m_{\mu\nu} , \\ &= a^2 \begin{pmatrix} -2\phi & \partial_i B + V_i \\ \partial_i B + V_i & -2\psi \delta_{ij} + h_{ij} \end{pmatrix} \\ \delta^n g_{\mu\nu} &= 0 , \quad (n = 2, 3, 4, \dots) , \end{aligned} \quad (\text{S1})$$

where the symbol $\delta^n g_{\mu\nu} = g_{\mu\nu}^{(n)}$ represents the n -th order perturbation of $g_{\mu\nu}$. ϕ and ψ are first order scalar perturbations. h_{ij} and V_i represent tensor perturbations and vector perturbations, respectively. Here, we have defined

$$h_{\mu\nu} = \begin{pmatrix} 0 & 0 \\ 0 & h_{ij} \end{pmatrix} , \quad m_{\mu\nu} = \begin{pmatrix} 0 & 0 \\ 0 & \delta_{ij} \end{pmatrix} , \quad V_\mu = (0, V_i) , \quad n_\mu = (-1, 0, 0, 0) , \quad n^\mu = (1, 0, 0, 0) . \quad (\text{S2})$$

To derive the vertex rules associated with multi-branch vertices, it is necessary to use the metric perturbations in Eq. (S1) to calculate the n -th order perturbation of the Einstein tensor. The Christoffel symbol can be expressed as

$$\Gamma_{\mu\nu}^\sigma = \frac{1}{2} g^{\sigma\alpha} (\partial_\nu g_{\alpha\mu} + \partial_\mu g_{\alpha\nu} - \partial_\alpha g_{\mu\nu}) . \quad (\text{S3})$$

The n -th order perturbation of the Christoffel symbol can be represented using the perturbations of the metrics $g_{\mu\nu}$ and $g^{\mu\nu}$

$$\begin{aligned} \delta^n \Gamma_{\mu\nu}^\sigma &= \frac{1}{2} (\delta^{n-1} g^{\sigma\alpha}) \delta (\partial_\nu g_{\alpha\mu} + \partial_\mu g_{\alpha\nu} - \partial_\alpha g_{\mu\nu}) + \frac{1}{2} (\delta^n g^{\sigma\alpha}) (\partial_\nu g_{\alpha\mu}^{(0)} + \partial_\mu g_{\alpha\nu}^{(0)} - \partial_\alpha g_{\mu\nu}^{(0)}) \\ &= \frac{1}{2} (\delta^{n-1} g^{\sigma\alpha}) [\partial_\nu (a^2 h_{\alpha\mu} - a^2 V_\mu n_\alpha - a^2 V_\alpha n_\mu - 2a^2 n_\alpha n_\mu \phi - 2a^2 \psi m_{\alpha\mu}) + \partial_\mu (a^2 h_{\alpha\nu} - a^2 V_\nu n_\alpha \\ &\quad - a^2 V_\alpha n_\nu - 2a^2 n_\alpha n_\nu \phi - 2a^2 \psi m_{\alpha\nu}) - \partial_\alpha (a^2 h_{\mu\nu} - a^2 V_\nu n_\mu - a^2 V_\mu n_\nu - 2a^2 n_\mu n_\nu \phi - 2a^2 \psi m_{\mu\nu})] \\ &\quad + a a' (\delta^n g^{\sigma\alpha}) (-\eta_{\alpha\mu} n_\nu - \eta_{\alpha\nu} n_\mu + \eta_{\mu\nu} n_\alpha) . \end{aligned} \quad (\text{S4})$$

In Eq. (S4), the metric perturbation $\delta^n g^{\sigma\alpha}$ can be straightforwardly determined from the relation $g^{\sigma\alpha} g_{\alpha\beta} = \delta_\beta^\sigma$. The explicit expression of $\delta^n g^{\sigma\alpha}$ is given by

$$\delta^n g^{\sigma\alpha} = \delta^n g_{ss}^{\sigma\alpha} + \delta^n g_{hh}^{\sigma\alpha} + \delta^n g_{sh}^{\sigma\alpha} + \delta^n g_{vv}^{\sigma\alpha} + \delta^n g_{sv}^{\sigma\alpha} + \delta^n g_{vh}^{\sigma\alpha} , \quad (\text{S5})$$

where

$$\delta^n g_{ss}^{\sigma\alpha} = \frac{2^n}{a^2} \left((-1)^{n+1} \phi^n n^\sigma n^\alpha + \psi^n m^{\sigma\alpha} \right) , \quad (\text{S6})$$

$$\delta^n g_{hh}^{\sigma\alpha} = \frac{(-1)^n}{a^2} \begin{cases} h_i^\alpha h^{\sigma i} , & n = 2 , \\ h_{bc} h^{\sigma b} h^{\alpha c} , & n = 3 , \\ h_b^{i_1} h_{i_1 c} h^{\sigma b} h^{\alpha c} , & n = 4 , \\ h_b^{i_1} h_c^{i_2} h_{i_1 i_2} h^{\sigma b} h^{\alpha c} , & n = 5 , \\ h_b^{i_1} h_c^{i_2} h_{i_1}^{i_3} h_{i_2}^{i_4} \dots h_{i_{n-5} i_{n-4}} h^{\sigma b} h^{\alpha c} , & n > 5 , \end{cases} \quad (S7)$$

$$\delta^n g_{sh}^{\sigma\alpha} = \begin{cases} 0 , & n = 1 , \\ \sum_{m=1}^{n-1} (-1)^m 2^m C_n^m \psi^m (\delta^{n-m} g_{hh}^{\sigma\alpha}) , & n > 1 , \end{cases} \quad (S8)$$

$$\delta^n g_{vv}^{\sigma\alpha} = \begin{cases} \frac{(-1)^{\frac{n-1}{2}}}{a^2} (V^i V_i)^{\frac{n-1}{2}} (V^\sigma n^\alpha + V^\alpha n^\sigma) , & n = \text{odd} , \\ \frac{1}{a^2} \left((-1)^{n/2} (V^i V_i)^{n/2-1} V^\alpha V^\sigma + (-1)^{n/2+1} (V^i V_i)^{n/2} n^\alpha n^\sigma \right) , & n = \text{even} , \end{cases} \quad (S9)$$

$$\delta^n g_{sv}^{\sigma\alpha} = \frac{1}{a^2} \begin{cases} 0 , & n = 1 , \\ 2 (V^\sigma n^\alpha + 2V^\alpha n^\sigma) (\psi - \phi) , & n = 2 , \\ 4 (V^\alpha n^\sigma + V^\sigma n^\alpha) (\phi^2 + \psi^2 - \phi\psi) + 2V^\alpha V^\sigma (\phi - 2\psi) \\ + 2V^\alpha V_\alpha n^\sigma n^\alpha (\psi - 2\phi) , & n = 3 , \\ 4V_b V^b (V^\alpha n^\sigma (\phi - \psi) + n^\alpha (V^\sigma (\phi - \psi) + n^\sigma (3\phi^2 - 2\phi\psi + \psi^2))) \\ + 8V^\alpha n^\sigma (-\phi^3 + \phi^2\psi - \phi\psi^2 + \psi^3) - 4V^\sigma (V^\alpha (\phi^2 - 2\phi\psi + 3\psi^2) \\ + 2n^\alpha (\phi^3 - \phi^2\psi + \phi\psi^2 - \psi^3)) , & n = 4 , \\ \dots\dots\dots , & \end{cases} \quad (S10)$$

$$\delta^n g_{vh}^{\sigma\alpha} = \frac{1}{a^2} \begin{cases} 0 , & n = 1 , \\ -V^b (h_b^\alpha n^\sigma + h_b^\sigma n^\alpha) , & n = 2 , \\ V^b (V^\alpha h_b^\sigma + V^\sigma h_b^\alpha + h_{bc} h^{\sigma c} n^\alpha + h_{bc} h^{\alpha c} n^\sigma) - V^b V^c h_{bc} n^\sigma n^\alpha , & n = 3 , \\ V^b (-V^\sigma h_{bc} h^{\alpha c} + V^\alpha h_{bc} (-h^{\sigma c} + V^c n^\sigma) - h_b^d h_{cd} (h^{\alpha c} n^\sigma + h^{\sigma c} n^\alpha) \\ + V^c (-h_b^\sigma h_c^\alpha + (V^\sigma h_{bc} + h_b^d h_{cd} n^\sigma) n^\alpha + V_b (h_c^\alpha n^\sigma + h_c^\sigma n^\alpha))) , & n = 4 , \\ \dots\dots\dots . & \end{cases} \quad (S11)$$

By utilizing the n -th order perturbation of the Christoffel symbol, we can directly derive the expression for the n -th order perturbation of the Ricci tensor $R_{\mu\nu}$, and subsequently determine the expression for the n -th

order perturbation of the Einstein tensor $G_{\mu\nu}$. The dominant contribution to induced gravitational waves often arises from source terms composed of scalar perturbations. Therefore, vertex diagrams formed by scalar perturbations are particularly important. If we only consider the scalar perturbations ψ and ϕ , the n -th order perturbations of $g^{\mu\nu}$ can be written as

$$\delta^n g^{\mu\nu} = \delta^n g_{ss}^{\mu\nu} = \frac{2^n}{a^2} \left((-1)^{n+1} \phi^n n^\mu n^\nu + \psi^n m^{\mu\nu} \right) = \frac{2^n}{a^2} \begin{pmatrix} (-1)^{n+1} \phi^n & 0 \\ 0 & \psi^n \delta^{ij} \end{pmatrix}. \quad (\text{S12})$$

In this case, Eq. (S4) can be simplified as

$$\begin{aligned} \delta^n \Gamma_{\mu\nu}^\sigma &= (-1)^n 2^{n-1} \left[m_{\mu\nu} (n^\sigma \phi^{n-1} (2\mathcal{H}\phi + 2\mathcal{H}\psi + \psi') + (-1)^n \psi^{n-1} \partial^\sigma \psi) + n^\sigma \phi^{n-1} (n_\nu \partial_\mu \phi - n_\mu n_\nu \phi' + n_\mu \partial_\nu \phi) \right. \\ &\quad \left. + (-1)^n \psi^{n-1} (n_\mu n_\nu \partial^\sigma \phi + m_\nu^\sigma n_\mu \psi' - m_\nu^\sigma \partial_\mu \psi + m_\mu^\sigma n_\nu \psi' - m_\mu^\sigma \partial_\nu \psi) \right]. \end{aligned} \quad (\text{S13})$$

The n -th order perturbation of Ricci tensor is given by

$$\begin{aligned} \delta^n R_{\mu\nu} &= \partial_\sigma \delta^n \Gamma_{\mu\nu}^\sigma - \partial_\nu \delta^n \Gamma_{\sigma\mu}^\sigma + \sum_{k=0}^n C_n^k (\delta^{n-k} \Gamma_{\sigma\alpha}^\sigma \delta^k \Gamma_{\mu\nu}^\alpha - \delta^{n-k} \Gamma_{\mu\alpha}^\sigma \delta^k \Gamma_{\sigma\nu}^\alpha) \\ &= (-1)^n 2^{n-1} \partial_\sigma \left[m_{\mu\nu} (n^\sigma \phi^{n-1} (2\mathcal{H}\phi + 2\mathcal{H}\psi + \psi') + (-1)^n \psi^{n-1} \partial^\sigma \psi) + n^\sigma \phi^{n-1} (n_\nu \partial_\mu \phi - n_\mu n_\nu \phi' + n_\mu \partial_\nu \phi) \right. \\ &\quad \left. + (-1)^n \psi^{n-1} (n_\mu n_\nu \partial^\sigma \phi + m_\nu^\sigma n_\mu \psi' - m_\nu^\sigma \partial_\mu \psi + m_\mu^\sigma n_\nu \psi' - m_\mu^\sigma \partial_\nu \psi) \right] \\ &\quad - 2^{n-1} \partial_\nu \left[n_\mu ((-1)^n \phi^{n-1} \phi' + 3\psi^{n-1} \psi') + (-1)^{n-1} \phi^{n-1} \partial_\mu \phi - 3\psi^{n-1} \partial_\mu \psi \right] \\ &\quad + C_n^k \left((-1)^{-k+n} 2^{-2+n} \phi^{-2-k} \psi^{-2-k} (-(-1)^k \phi^{k+n} \psi^{2+k} \phi' (m_{\mu\nu} (2\mathcal{H}\phi + 2\mathcal{H}\psi + \psi') + n_\nu \partial_\nu \phi) \right. \\ &\quad \left. - 3(-1)^n \phi^{1+2k} \psi^{1+n} (m_{\mu\nu} (\psi'^2 + 2\mathcal{H}\phi\psi' + 2\mathcal{H}\psi\psi') + n_\nu \psi' \partial_\mu \phi) - 3(-1)^{k+n} \phi^{2+k} \psi^{k+n} \right. \\ &\quad \left. (m_{\mu\nu} \partial_\alpha \psi \partial^\alpha \psi + \partial_\mu \psi (n_\mu \psi' - 2\partial_\mu \psi)) + (-1)^{2k} \phi^{1+n} \psi^{1+2k} (-m_{\mu\nu} \partial_\alpha \psi \partial^\alpha \phi + \partial_\mu \psi \partial_\nu \phi + \partial_\mu \phi n_\nu \phi'^2 - \partial_\mu \phi \phi' \partial_\nu \phi) \right. \\ &\quad \left. + n_\mu (3(-1)^n \phi^{1+2k} \psi^{1+n} \psi' n_\nu \phi' - \psi' \partial_\nu \phi + (-1)^k \phi^{k+n} \psi^{2+k} (n_\nu \phi'^2 - \phi' \partial_\nu \phi) \right. \\ &\quad \left. - (-1)^{2k} \phi^{1+n} \psi^{1+2k} (n_\nu \partial_\alpha \phi \partial^\alpha \phi + \psi' \partial_\nu \phi) - 3(-1)^{k+n} \phi^{k+n} \psi^{k+n} (n_\nu \partial_\alpha \psi \partial^\alpha \phi + \psi' \partial_\nu \psi) \right) \\ &\quad (-1)^{-k+n} 2^{-2+n} \phi^{-1-k} \psi^{-1-k} \left((-1)^{k+1} \phi^n \psi^{1+k} \left((-1)^k \psi^4 (m_{\mu\nu} (\psi'^2 + 2\mathcal{H}(\phi + \psi) \psi') \right. \right. \\ &\quad \left. \left. + m_{\mu\alpha} n_\nu (2\mathcal{H}(\phi + \psi) + \psi') \partial^\alpha \phi) + \phi^4 \partial_\mu \phi (n_\nu \phi' - \partial_\nu \phi) \right) \right. \\ &\quad \left. + n_\mu (-(-1)^k \phi^n \psi^{1+k} (\phi^4 (-n_\nu \phi'^2 + \phi' \partial_\nu \phi) + (-1)^k \psi^4 (n_\nu \partial_\alpha \phi \partial^\alpha \phi + \psi' \partial_\nu \phi)) + \right. \\ &\quad \left. (-1)^n \phi^{1+k} \psi^n (-\phi^4 (m_{\nu\alpha} (2\mathcal{H}(\phi + \psi) + \psi') + n_\nu \partial_\alpha \phi) \partial^\alpha \phi + (-1)^k \psi^4 (3n_\nu \psi'^2 + \psi' (m_{\nu\alpha} \partial^\alpha \psi - 4\partial_\nu \psi))) \right) \\ &\quad \left. + (-1)^n \phi^{1+k} \psi^n (-\phi^4 (m_{\mu\nu} (\psi'^2 + 2\mathcal{H}\phi\psi' + 2\mathcal{H}\psi\psi') + n_\nu \psi' \partial_\mu \phi) + \right. \\ &\quad \left. (-1)^k \psi^4 (-2m_{\mu\nu} \partial_\alpha \psi \partial^\alpha \psi - \partial_\mu \psi (4n_\nu \psi' + m_{\nu\alpha} \partial^\alpha \psi - 6\partial_\nu \psi) + m_{\mu\alpha} \partial^\alpha \psi (n_\nu \psi' - \partial_\nu \psi + m_{\nu\sigma} \partial^\sigma \psi))) \right). \end{aligned} \quad (\text{S14})$$

The n -th order perturbation of the Einstein tensor can be expressed as follows

$$\delta^n G_{\mu\nu} = \delta^n R_{\mu\nu} - \frac{1}{2} \left(g_{\mu\nu}^{(0)} \delta R + \delta g_{\mu\nu} \delta^{n-1} R \right), \quad (\text{S15})$$

where

$$\delta^n R = \delta^n (g^{\mu\nu} R_{\mu\nu}) = \sum_{k=0}^n C_n^k \frac{2^{n-k}}{a^2} \left((-1)^{n-k+1} \phi^{n-k} n^\mu n^\nu + \psi^{n-k} m^{\mu\nu} \right) \delta^k R_{\mu\nu}. \quad (\text{S16})$$

During the radiation-dominated era, we set $\delta^n p = \frac{1}{3} \delta^n \rho$. The energy-momentum tensor of perfect fluid can be written as

$$T_{\mu\nu} = \frac{4}{3} \rho u_\mu u_\nu + \frac{1}{3} \rho g_{\mu\nu}. \quad (\text{S17})$$

The n -th order perturbation of $T_{\mu\nu}$ is given by

$$\delta^n T_{\mu\nu} = \frac{4}{3} \sum_{m=0}^n \sum_{l=0}^m C_n^m \delta^{n-m} \rho C_m^l \delta^{m-l} u_\mu \delta^l u_\nu + \frac{1}{3} \sum_{m=0}^n C_n^m \delta^{n-m} g_{\mu\nu} \delta^m \rho . \quad (\text{S18})$$

By utilizing the time-time component and the time-space component of the n -th order perturbations of Einstein's field equation, we can represent density perturbations $\delta^n \rho$ and velocity perturbations $\delta^n u_\mu$ as metric perturbations. Substituting the calculated density and velocity perturbations into the space-space component of the n -th order perturbations of Einstein's field equations yields the source terms associated with various vertex diagrams.

TWO-BRANCH VERTEX

We present the specific expressions for the source terms corresponding to all the 2-branch vertices of the induced gravitational waves. In the vertex diagrams, the dashed lines, wavy lines and spring-like lines represent scalar, vector, and tensor perturbations, respectively.

(1) Induced gravitational waves sourced by lower-order scalar perturbations ϕ and ψ .

$$\begin{aligned} \mathcal{S}_{\phi\phi,ij} + \mathcal{S}_{\psi\phi,ij} + \mathcal{S}_{\psi\psi,ij} = & \partial_i \psi \partial_j \phi + \frac{\partial_i \psi' \partial_j \phi}{\mathcal{H}} + \partial_i \phi \partial_j \psi - 3 \partial_i \psi \partial_j \psi + \frac{\partial_i \phi \partial_j \psi}{\mathcal{H}} + \frac{\partial_i' \psi \partial_j' \psi}{\mathcal{H}^2} \\ & - 2 \phi \partial_j \partial_i \phi - 2 \psi \partial_j \partial_i \psi . \end{aligned} \quad (\text{S19})$$

For example, if we need to calculate the source term of the 10th-order gravitational waves induced by the

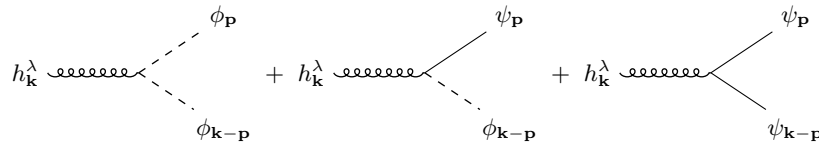


FIG. S1: The 2-branch vertex diagram of higher-order gravitational waves induced by the product of two lower-order scalar perturbations.

product of two 5th-order scalar perturbations, we only need to make the following substitution in the source term of Eq. (S19): $\phi \rightarrow \frac{1}{5!} \phi^{(5)}$, $\psi \rightarrow \frac{1}{5!} \psi^{(5)}$.

(2) Induced gravitational waves sourced by lower-order vector perturbation V_i .

$$\mathcal{S}_{VV,ij} = -\frac{1}{2} V^b \partial_b \partial_i V_j - \frac{1}{2} V^b \partial_b \partial_j V_i + \frac{1}{2} \partial_b V_j \partial^b V_i + \frac{\partial_b \partial^b V_i \partial_c \partial^c V_j}{16 \mathcal{H}^2} + \frac{1}{2} \partial_i V^b \partial_j V_b + V^b \partial_j \partial_i V_b . \quad (\text{S20})$$

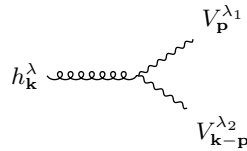


FIG. S2: The 2-branch vertex diagram of higher-order gravitational waves induced by the product of two lower-order vector perturbations.

(3) Induced gravitational waves sourced by lower-order tensor perturbation h_{ij} .

$$\begin{aligned} \mathcal{S}_{hh,ij} = & \frac{1}{2}h'_i h'_{jb} - \frac{1}{2}h^{bc}\partial_c\partial_b h_{ij} + \frac{1}{2}h^{bc}\partial_c\partial_i h_{jb} + \frac{1}{2}h^{bc}\partial_c\partial_j h_{ib} + \frac{1}{2}\partial_b h_{jc}\partial^c h_i^b - \frac{1}{2}\partial_c h_{jb}\partial^c h_i^b \\ & - \frac{1}{4}\partial_i h^{bc}\partial_j h_{bc} - \frac{1}{2}h^{bc}\partial_j\partial_i h_{bc} . \end{aligned} \quad (\text{S21})$$

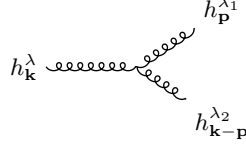


FIG. S3: The 2-branch vertex diagram of higher-order gravitational waves induced by the product of two lower-order tensor perturbations.

(4) Induced gravitational waves sourced by lower-order tensor perturbation h_{ij} and lower-order scalar perturbations ϕ and ψ .

$$\begin{aligned} \mathcal{S}_{h\phi,ij} + \mathcal{S}_{h\psi,ij} = & h''_{ij}\phi + 2h'_{ij}\mathcal{H}\phi + \frac{1}{2}h'_{ij}\phi' - 2h_{ij}\mathcal{H}\phi' - \frac{1}{2}h'_{ij}\psi' - 8h_{ij}\mathcal{H}\psi' - 3h_{ij}\psi'' + \psi\partial_b\partial^b h_{ij} \\ & - h_{ij}\partial_b\partial^b\phi + \frac{8}{3}h_{ij}\partial_b\partial^b\psi - h^b{}_i\partial_b\partial_i\psi - h^b{}_i\partial_b\partial_j\psi + \frac{1}{2}\partial_b h_{ij}\partial^b\phi + \frac{3}{2}\partial_b h_{ij}\partial^b\psi - \frac{1}{2}\partial^b\phi\partial_i h_{jb} \\ & - \frac{1}{2}\partial^b\psi\partial_i h_{jb} - \frac{1}{2}\partial^b\phi\partial_j h_{ib} - \frac{1}{2}\partial^b\psi\partial_j h_{ib} . \end{aligned} \quad (\text{S22})$$

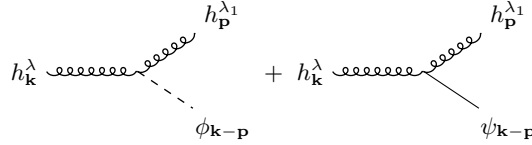


FIG. S4: The 2-branch vertex diagram of higher-order gravitational waves induced by the product of lower-order tensor perturbations and lower-order scalar perturbations.

(5) Induced gravitational waves sourced by lower-order vector perturbation V_i and lower-order scalar perturbations ϕ and ψ .

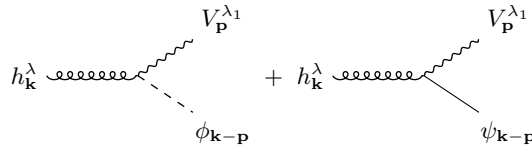


FIG. S5: The 2-branch vertex diagram of higher-order gravitational waves induced by the product of lower-order vector perturbations and lower-order scalar perturbations.

$$\begin{aligned}
\mathcal{S}_{V\phi,ij} + \mathcal{S}_{V\psi,ij} = & -2\mathcal{H}\phi\partial_i V_j - \frac{1}{2}\phi'\partial_i V_j - \frac{1}{2}\psi'\partial_i V_j - \phi\partial_i V_j' - \frac{\partial_b\partial^b V_j\partial_i\phi}{4\mathcal{H}} + V_j'\partial_i\psi + 2V_j\mathcal{H}\partial_i\psi + V_j\partial_i\psi' \\
& - \frac{\partial_b\partial^b V_j\partial_i\psi'}{4\mathcal{H}^2} - 2\mathcal{H}\phi\partial_i V_j - \frac{1}{2}\phi'\partial_i V_j - \frac{1}{2}\psi'\partial_i V_j - \phi\partial_i V_j' - \frac{\partial_b\partial^b V_j\partial_i\phi}{4\mathcal{H}} + V_j'\partial_i\psi + 2V_j\mathcal{H}\partial_i\psi \\
& + V_j\partial_i\psi' - \frac{\partial_b\partial^b V_j\partial_i\psi'}{4\mathcal{H}^2} .
\end{aligned} \tag{S23}$$

(6) Induced gravitational waves sourced by lower-order vector perturbation V_i and lower-order tensor perturbation h_{ij} .

$$\begin{aligned}
\mathcal{S}_{Vh,ij} = & \frac{1}{2}V^{b'}\partial_b h_{ij} + V^b\mathcal{H}\partial_b h_{ij} + V^b\partial_b h'_{ij} - \frac{1}{2}h'_{jb}\partial^b V_i - \frac{1}{2}h'_{ib}\partial^b V_j - \frac{1}{2}V^{b'}\partial_i h_{jb} - V^b\mathcal{H}\partial_i h_{jb} - \frac{1}{2}V^b\partial_i h'_{jb} \\
& - \frac{1}{2}V^{b'}\partial_j h_{ib} - V^b\mathcal{H}\partial_j h_{ib} - \frac{1}{2}V^b\partial_j h'_{ib} .
\end{aligned} \tag{S24}$$

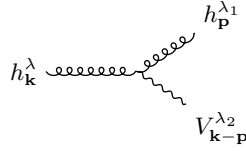


FIG. S6: The 2-branch vertex diagram of higher-order gravitational waves induced by the product of lower-order tensor perturbations and lower-order vector perturbations.

THIRD-ORDER TENSOR-SCALAR INDUCED GRAVITATIONAL WAVES

The explicit expression of $h_{\mathbf{k},sh_{sh}}^{\lambda,(3)}$ is given by

$$\begin{aligned}
h_{sh_{sh}}^{\lambda,(3)}(\eta, \mathbf{k}) = & \frac{16}{3} \int \frac{d^3 p}{(2\pi)^{3/2}} \int \frac{d^3 q}{(2\pi)^{3/2}} \varepsilon^{\lambda,lm}(\mathbf{k}) \varepsilon_{lm}^{\lambda_1}(\mathbf{p}) \varepsilon^{\lambda_1,ij}(\mathbf{p}) \varepsilon_{ij}^{\lambda_2}(\mathbf{q}) v^2 \\
& \times \int_0^{\bar{x}} d\bar{x} \frac{\bar{x}}{x} \sin(x - \bar{x}) f_{sh_{sh}}^{(3)}(u, v, \bar{u}, \bar{v}, \bar{x}) \zeta_{\mathbf{k}-\mathbf{p}} \zeta_{\mathbf{p}-\mathbf{q}} \mathbf{h}_{\mathbf{q}}^{\lambda_2} .
\end{aligned} \tag{S25}$$

In Eq. (S25), $f_{sh_{sh}}^{(3)}(u, v, \bar{u}, \bar{v}, x)$ can be represented as

$$\begin{aligned}
f_{sh_{sh}}^{(3)}(u, v, \bar{u}, \bar{v}, x) = & -2T_\phi(ux) f_{sh}^{(2)}(\bar{u}, \bar{v}, y) + T_\phi(ux) p^2 I_{sh}^{(2)}(\bar{u}, \bar{v}, y) - \frac{u}{v^2 x} p^2 I_{sh}^{(2)}(\bar{u}, \bar{v}, y) \frac{d}{d(ux)} T_\phi(ux) \\
& + \frac{u^2}{3v^2} T_\phi(ux) p^2 I_{sh}^{(2)}(\bar{u}, \bar{v}, y) + \frac{(1-v^2-u^2)}{2v^2} T_\phi(ux) p^2 I_{sh}^{(2)}(\bar{u}, \bar{v}, y) ,
\end{aligned} \tag{S26}$$

where

$$\begin{aligned}
f_{sh}^{(2)}(\bar{u}, \bar{v}, y) = & \frac{10u}{x} \frac{d}{d(ux)} T_\phi(ux) T_h(vx) + 3u^2 \frac{d^2}{d(ux)^2} T_\phi(ux) T_h(vx) + \frac{5}{3} u^2 T_\phi(ux) T_h(vx) \\
& + (1-v^2-u^2) T_\phi(ux) T_h(vx) + 2v^2 T_\phi(ux) T_h(vx) , \\
p^2 I_{sh}^{(2)}(\bar{u}, \bar{v}, y) = & 4 \int_0^y d\bar{y} \left(\frac{\bar{y}}{y} \sin(y - \bar{y}) f_{sh}^{(2)}(\bar{u}, \bar{v}, \bar{y}) \right) , \\
T_\phi(x) = & \frac{9}{x^2} \left(\frac{\sqrt{3}}{x} \sin\left(\frac{x}{\sqrt{3}}\right) - \cos\left(\frac{x}{\sqrt{3}}\right) \right) .
\end{aligned}$$

We have defined $|\mathbf{k} - \mathbf{p}| = u|\mathbf{k}|$, $|\mathbf{p}| = v|\mathbf{k}|$, $|\mathbf{p} - \mathbf{q}| = \bar{u}|\mathbf{p}|$, $x = |\mathbf{k}|\eta$, and $y = |\mathbf{p}|\eta$.